# Autonomous Inspection of Electrical Transmission Structures with Airborne UV Sensors and Automated Air Traffic Management

Andrew J. Moore[1]
*Dynamic Systems and Controls Branch, NASA Langley Research Center, Hampton, VA, 23681*

Matthew Schubert[2]
*Analytical Mechanics Associates, Inc., Hampton, VA, 23666*

and

Nicholas Rymer[3]
*National Institute of Aerospace, Hampton, VA, 23666*

**This report details test and measurement flights to demonstrate autonomous UAV inspection of high-voltage electrical transmission structures. A UAV built with commercial, off-the-shelf hardware and software, supplemented with custom sensors and logging software, measured ultraviolet emissions from a test generator placed on a low-altitude substation and a medium-altitude switching tower. Since corona discharge precedes catastrophic electrical faults on high-voltage structures, detection and geolocation of ultraviolet emissions is needed to develop a UAV-based self-diagnosing power grid.**

**Signal readings from an onboard ultraviolet sensor were validated during flight with a commercial corona camera. Geolocation was accomplished with onboard GPS; the UAV position was logged to a local ground station and transmitted in real time to a NASA server for tracking in the national airspace. The method has practicality and relevance but not adequacy; either improved UAV position determination technology or increased sensor range is needed to enable broad deployment of this method.**

## I. Nomenclature

| | | |
|---|---|---|
| *dGPS* | = | differential GPS |
| *kV* | = | thousands of volts |
| *sGPS* | = | single-ended GPS |

## II. Introduction

Manually piloted UAVs have been deployed routinely to inspect high-voltage electrical transmission lines in recent years [1][2][3][4], and a variety of sensors and concepts for autonomous transmission line inspection have been proposed (see [5][6] for reviews). One or more manual flights to test sensors, operational concepts, and autonomy methods are needed to verify a particular UAV platform; commonly at least one manual flight within a given flight corridor is undertaken to determine inspection poses and to cope with site-specific geography. Once a site is surveyed and waypoints along an effective flight inspection corridor are determined, autonomous UAV flights can economically reinspect a line section repeatedly. The work described in this report follows in that same sequence: exploratory manual flights are followed by autonomous flights at two de-energized high-voltage infrastructure locations.

[1] Aerospace Technologist, NASA Langley Research Center, 8 Langley Blvd., MS 308, Hampton VA, USA, 23681.
[2] Programmer 3, Analytical Mechanics Associates, 21 Enterprise Parkway, Suite 300, Hampton, VA 23666.
[3] Research Scientist, National Institute of Aerospace, 100 Exploration Way, Hampton VA, USA, 23666.

Most of the technologies described herein are broadly applicable to UAV deployment. In addition, this report describes results obtained from a compact UV sensor package developed at NASA Langley that is specifically applicable to high-voltage fault detection. In electrical power transmission, great care is taken to avoid sharp protrusions on high-voltage structures; electron avalanches from high-potential points produce, via impact ionization and subsequent recombination of atmospheric plasma, an ultraviolet (UV) photon spray called coronal discharge [7]. While most coronas are benign, some are indicative of a severe degradation that requires immediate attention; location, diagnosis, and disposition of coronas are necessary components of transmission line inspection. The core technology, a sensor based on the photoelectric effect and gas multiplication [8], is solar blind and has a wide field of view. An early version of this sensor was calibrated against a 100 kV corona [9]; subsequent versions are more sensitive, allowing a greater standoff distance from the high-voltage structure.

Since it is very lightweight, this technology can be mounted on the UAV. If the sensitivity is high enough to allow a sufficient standoff distance, a fleet of UAVs equipped with compact UV sensors could autonomously inspect high-voltage structures and locate faults that may result in a power outage. If distributed across a power grid (for example, at substations), this fleet could serve as the detection component of a self-diagnosing power grid (Figure 1). Imagery and other telemetry from the UAV deployments could then be interpreted remotely by experienced grid operation and line crews, enabling the rapid dispatch of a nearby line crew in a repair truck loaded with the components necessary to repair the fault.

Two series of high voltage infrastructure inspection flights are detailed in this report. The flights demonstrate the applicability of compact UV sensors for finding transmission line faults and document the fidelity of UV sensing with an independent sensor. However, due to the limited range of compact sensors with no optical augmentation combined with inaccuracies in UAV positioning, it was not possible to demonstrate that the method is adequate for this task. Either increased sensor range or improved UAV position determination technology is needed to enable broad deployment of this method.

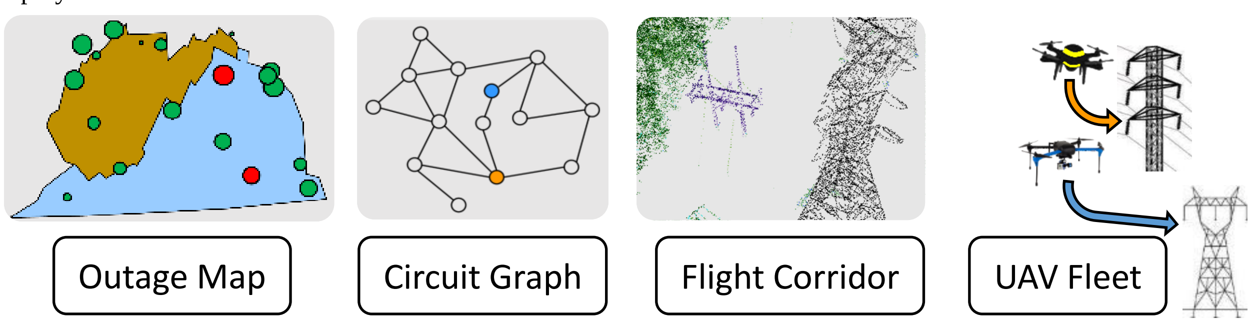


**Figure 1. Components of a self-diagnosing power grid. UAVs cached at locations across the grid, such as electrical substations, can be deployed on demand to locate and characterize the faults based on geographic outage maps and topological circuit maps.**

## III. Test and Measurement Flights

### A. Overview

Two days of experimental UAV flights were conducted at Dominion Virginia Power's Chester training facility on November 7 and 8, 2016. A variety of commercial transmission structures, de-energized for training purposes, are located at this facility. The UAV was built with commercial, off-the-shelf hardware and software, supplemented with custom sensor logging software. Twelve test flights with increasing instrumentation validated the measurement methods at two structures: a low-altitude substation, and a medium-altitude switching tower. At the site of each structure, manual flights were conducted first, in preparation for a waypoint-based autonomous flight.

A corona generator was placed on each structure, with a coronal UV intensity strength set to produce a signal measurable by a pair of onboard ultraviolet sensors. The UAV distance from the generator was no closer than 12' for manual flights, and no closer than 20' for autonomous flights. To validate sensor records, visible and ultraviolet imagery of the flight path was recorded.

UAV position was tracked by the onboard autopilot and saved to a ground computer after the flights each day. In addition, the UAV position was forwarded during the flight from the ground station computer to a NASA UAS Traffic Management (UTM) [10] server for real-time traffic management. After all flight data capture and recording technologies were operating successfully, as proven in test flights, measurement flights were conducted at the two locations. These flights demonstrated, for the first time, an autonomously guided UAV with onboard compact UV sensors recording signals directly relevant to transmission line fault geolocation, while tracked in the national airspace. A more detailed report [9] details each flight and the hardware and software components employed.

Flight locations within the Chester training facility are shown in Figure 2. The substation is a recently added structure at the east side of the facility, and the switching tower is at the far north side, close to Old Stage Road in Chester, Virginia. The video and corona cameras were placed 200 to 300 feet from the flight locations to accommodate the small depth of field of the corona camera. Test flights took place on the first day and the morning of the second day, and measurement flights took place in the afternoon of the second day. Designated according to the structure, day, and flight count,[4] the set of experimental flights was comprised of a substation flight series S1_1 through S2_5 and a tower flight series T1_1 through T2_4.

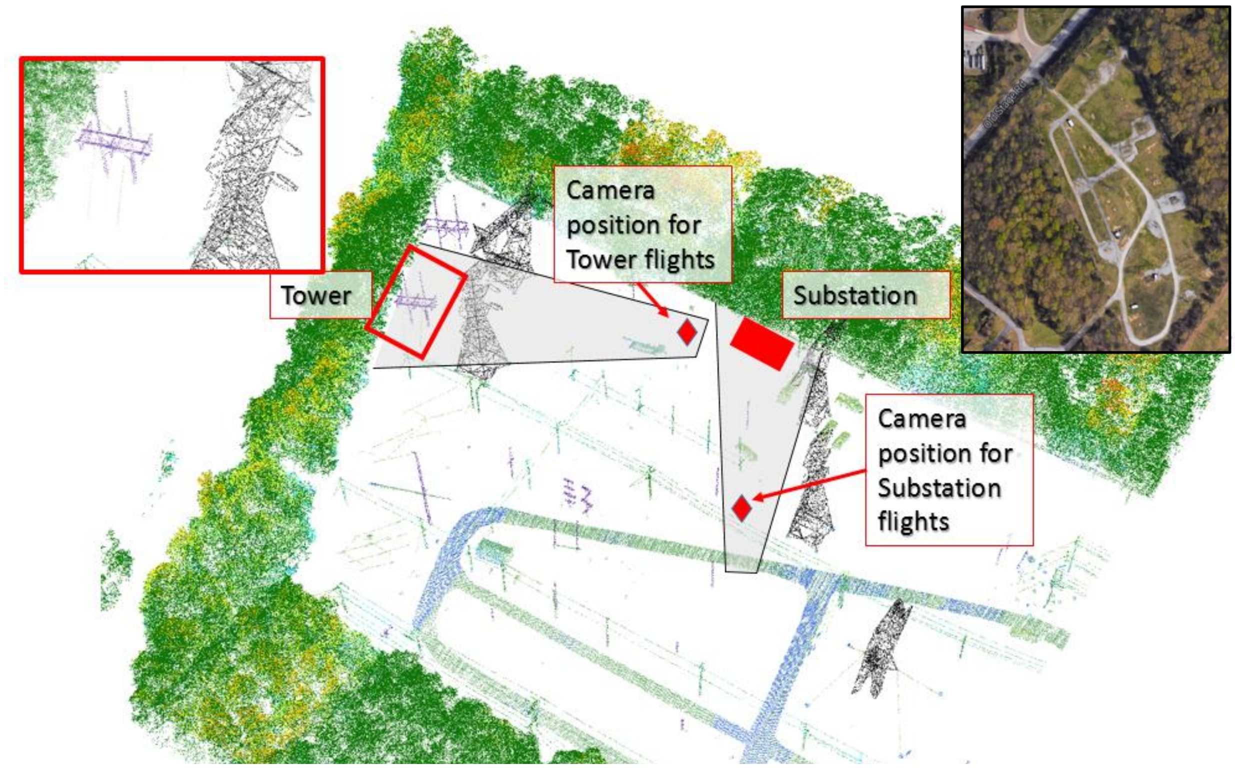


**Figure 2. Chester Virginia flight range. Flight and camera positions superimposed on Dominion-provided lidar. The flight locations and camera recording positions for the substation and tower flights were in the northeast corner of the range. A close-up of the switching tower is shown in the top left inset, and a satellite image of the facility (for which up is north) is shown in the top right inset. ©*Lidar data: Dominion Virginia Power; Map data: Google, DigitalGlobe & NASA***

## B. Substation Test and Measurement Flights

Low-altitude flight maneuvers and sensor checks were accomplished in the substation (S) test flights (top of Table 1). After a free-ranging manual flight S1_1 that approached as close as 12 feet to the target location, the corona source was energized and the UV sensors were tested in autonomous flights S1_2 and S1_3, which approached as close as 20 feet to the target location. Figure 3 illustrates the physical interpretation of the UV plots in this report, using as an example the L-shaped S1_3 flight path. Since the corona sensors were on the sides of the UAV, the left (port) sensor detected corona during the first leg, and the right (starboard) sensor detected corona during the second leg. The waypoints used in flight S1_2 did not completely sweep in front of the source, and so the third waypoint was moved further north. The effectiveness of this waypoint adjustment may be seen by comparing the S1_2 and S1_3 rows of Figure 4.

---

[4] SD_R (S=Substation, D=Day, R=Repetition) and TD_R (T=Tower, D=Day, R=Repetition)

Waypoint placement and sensor functionality was verified in back-and-forth manual flight S2_1 in front of the substation structure. In this flight, the UAV was kept oriented north so that it was flying forward and then backward multiple times; several peaks of signal strength (which correspond to points of nearest approach) are seen from the right sensor in the S2_1 UV plot in Figure 4. Flight path transmission to the NASA UTM server was tested during this flight.

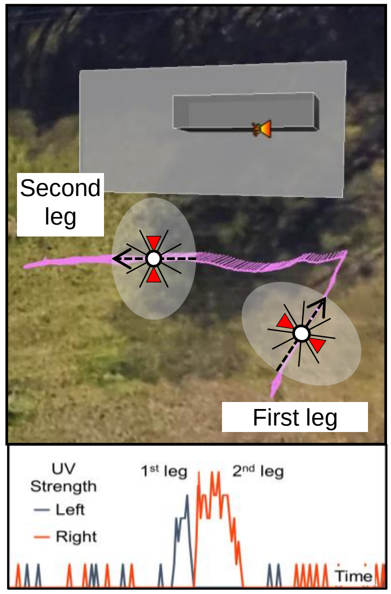


**Figure 3. Spatial validation of the signals from port (left) and starboard (right) compact UV sensors. The substation structure and its concrete pad, visible in Figure 6 below, were built after available satellite imagery was archived, so they are rendered manually in this image as gray rectangles. The corona generator location is indicated by an orange icon.** ***©Map data: Google, DigitalGlobe & NASA***

Finally, corona camera recording and UTM flight path transmission was conducted in the trio of autonomous measurement flights S2_3, S2_4, and S2_5 (Figure 5 and bottom of Table 1). The UAV altitude was varied in these three flights both to determine the altitude needed to frame it in the limited field of view of the corona camera and to test UTM altitude recording fidelity. Altitudes of 9.8 feet (3 meters; flight S2_3) and 16.4 feet (5 meters; flight S2_4) were too low and too high, respectively, to capture the UAV within the tight corona camera field of view, but an altitude of 13.1 feet (4 meters; flight S2_5) produced corona camera video imagery that independently validated the corona signal detected by the onboard sensor (Figure 6). Postflight analysis revealed that while the UTM latitude and longitude records were accurate, the altitude record was distorted (right column of Figure 5) and this discrepancy was reported to the corresponding software development team.

**Table 1. Substation test and measurement flights**

| **Substation Test Flights** | | | | | | |
|---|---|---|---|---|---|---|
| Flight | Description | UV Plot | Flight path | UV Image | Visible Image | UTM path |
| S1_1 | 1st manual flight | | ✓ | | | |
| S1_2 | 1st auton. flight | ✓ | ✓ | | ✓ | |
| S1_3 | 2nd auton. flight | ✓ | ✓ | | ✓ | |
| S2_1 | 1st manual flight | ✓ | ✓ | | ✓ | ✓ |
| **Substation Measurement Flights** | | | | | | |
| Flight | Description | UV Plot | Flight path | UV Image | Visible Image | UTM path |
| S2_3 | 2nd auton. flight | | ✓ | | | ✓ |
| S2_4 | 3rd auton. flight | ✓ | ✓ | | | ✓ |
| S2_5 | 4th auton. flight | ✓ | ✓ | ✓ | ✓ | ✓ |

| Flight and Description | UV Plot | Flight Path |
|---|---|---|
| S1_1<br>1st manual<br>flight | N/A |  |
| S1_2<br>1st auton.<br>flight | 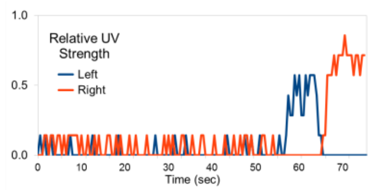 | 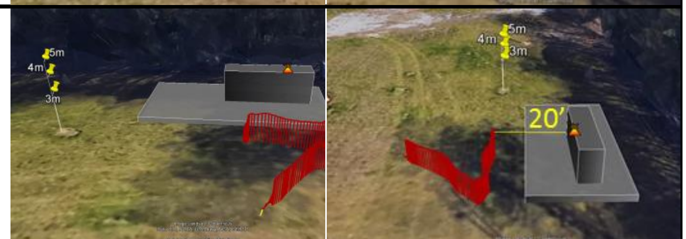 |
| S1_3<br>2nd auton.<br>flight | 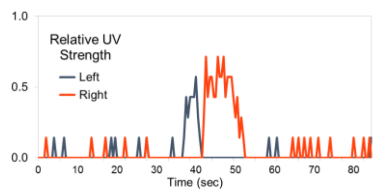 |  |
| S2_1<br>1st manual<br>flight | 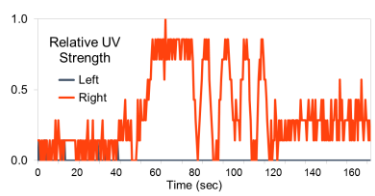 | 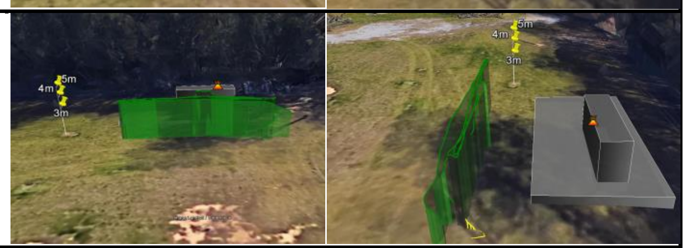 |

**Figure 4. UV signal and flight path plots for the four substation test flights. The approximate distance to the corona generator (12' or 20') is indicated for the first three flights, which verified the compact UV sensor response. The substation structure and its concrete pad, visible in Figure 6 below, were built after available satellite imagery was archived, so they are rendered manually in this image as gray rectangles. The corona generator location is indicated by an orange icon. ©*Map data: Google, DigitalGlobe & NASA***

| Flight | Alti-tude (m) | UV Plot | Autopilot Flight Paths (overlay) | UTM Flight Path |
|---|---|---|---|---|
| S2_3 | 3 | N/A | 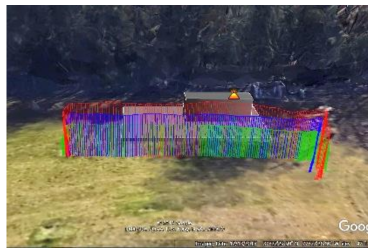 |  |
| S2_4 | 5 | 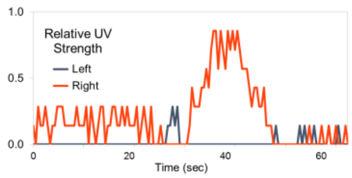  | 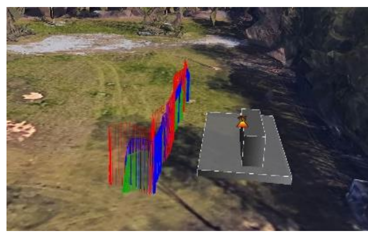 |  |
| S2_5 | 4 | 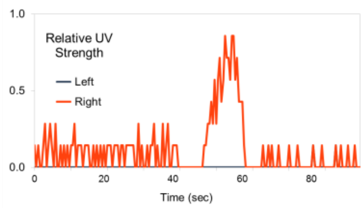  | |  |

**Figure 5. Altitude, UV signal and flight path plots for the three substation measurement flights. Both autopilot and UTM flight paths are shown; autopilot flight paths for all three flights are overlaid in the center column, showing flight paths with three altitudes (3, 5, and 4 meters colored green, red, and blue) in frontal and lateral views. The UTM flight paths (right column) are shown individually for each flight in frontal view. ©*Map data: Google, DigitalGlobe & NASA***

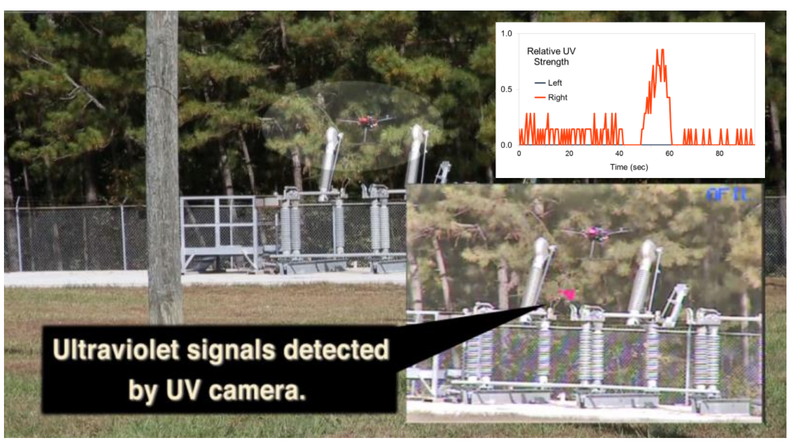


**Figure 6. Validation of the compact UV sensor signal with corona camera in a substation measurement flight S2_5. The visible camera image shows the UAV above the substation structure (background; UAV is in lightened ellipse). The inset at top right shows the compact UV sensor recording, which reaches a maximum as the UAV passes the corona generator. The inset at bottom right shows the corona camera record; the bright red blobs at the center of the image are locations of UV emission.**

## C. Switching Tower Test and Measurement Flights

In a similar manner, a series of test flights were executed in proximity to a corona generator mounted at a height of 30 feet on a switching tower. In these test flights waypoints for autonomous flight were determined, UV corona sensing was verified, and communications were configured for UTM recording (see [9] for details). The tower flight series culminated in the fully instrumented autonomous measurement flight T2_4. Two waypoints were used, one to the west and one to east of the tower. Onboard UV sensors recorded the generated corona (Figure 7) as verified with the ground-based corona camera (Figure 8). The UAV flight path was transmitted to a remote NASA UTM server (Figure 7). Success at the altitude of the switching tower confirmed the practicality of the UAV-based method for corona inspection of transmission line infrastructure.

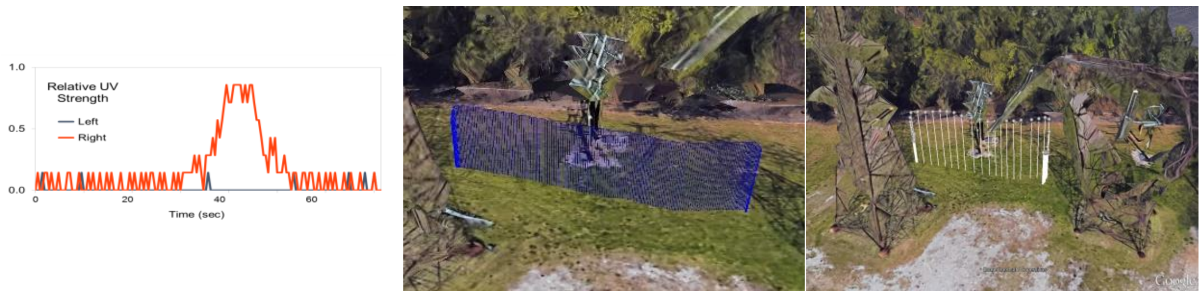


**Figure 7. Switching tower measurement flight T2_4. The compact UV sensor readings during the flight are plotted at left, the autopilot flight path is shown at middle, and the UTM flight record is shown at right. Corona generator placement is shown in Figure 8. ©*Map data: Google, DigitalGlobe & NASA***

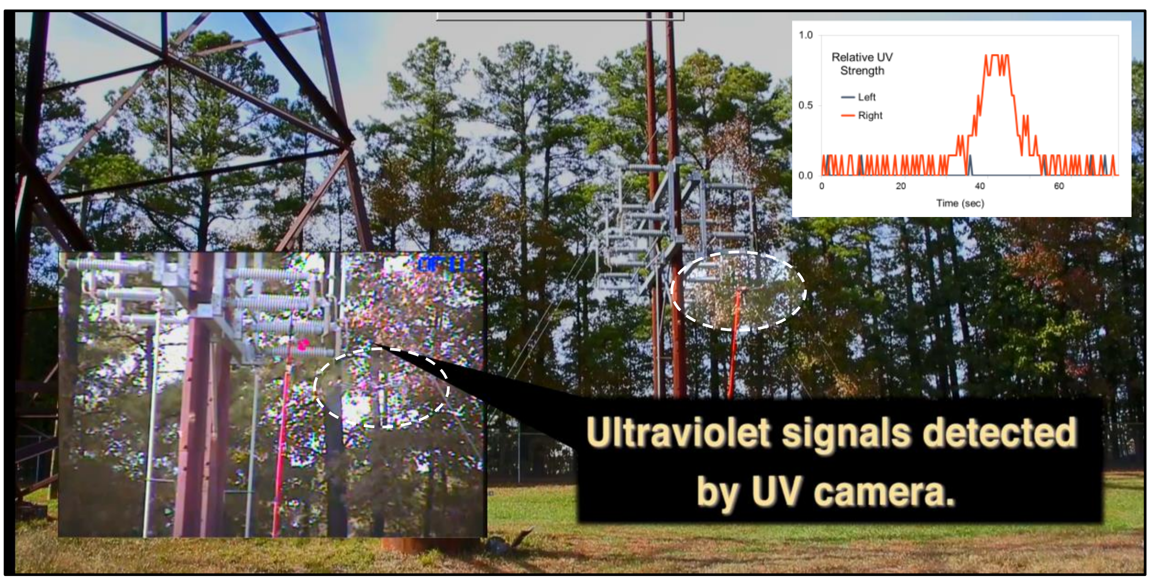


**Figure 8. Validation of the compact UV sensor signal with corona camera in tower measurement flight T2_4. The corona camera imagery (inset at left) verifies the UV sensor result (inset at top right). The UAV is framed in a low-contrast oval (white dashed outline) in this imagery. The bright red blobs at the center of the corona camera image are locations of UV emission.**

# IV. Discussion

## A. Compact sensor technology and standoff distance

The UAV was built with commercial, off-the-shelf hardware and software, supplemented with custom sensor logging software. The base aircraft platform cost was less than $5K, and commercial laptops were used as ground stations. One consequence of this low-cost approach is that UAV positional accuracy is too low to allow precision autonomous flights. The test signal was increased to compensate for this deficiency. In this section, the experimental approach and caveats about interpretation of the results are detailed.

1. *Leveraging new sensor and UAV technology development*

Compact UV sensors promise to supplement or replace corona cameras for finding potential high-voltage transmission line faults [1]. Corona camera adoption is limited, at least in part, due to camera size, cost, and fragility; compact UV sensor technology is superior in all three of these measures of market fitness. However, corona cameras have exquisite sensitivity to the weak UV photon flux density produced by coronas. They are so sensitive that a user with limited training can spot a corona from the ground at a distance of 300 feet or more. In contrast, compact UV sensors must be located within a few yards of a corona to sense it reliably.

As a result, compact UV sensors have not been applied in transmission line inspection. Two recent technology advances may change this: an increased sensor sensitivity, and the broad deployment of UAVs that can deliver the sensor very close to the corona source.

2. *Device sensitivity and range*

Figure 9 shows the improvement in sensitivity of a commercial line of UV sensors [11] that use the photoelectric effect to sense narrow-band UV photons in a Geiger-Mueller tube and circuit configuration. The leftmost model was calibrated experimentally at the Electric Power Research Institute in July of 2015 to determine detectability of a 100 kV corona. The device (R9533, at left) has to be within four feet of the discharge to reliably report a signal corresponding to a 100 kV corona (four foot maximum detection distance). Its successor (R1753-01, at middle) is twice as sensitive in our laboratory tests (eight foot maximum detection distance from a 100 kV corona). In 2016, a new design (R13192, at right) yielded an additional 50% higher sensitivity (twelve foot maximum detection distance from a 100 kV corona). Laboratory measurements of the third generation device are shown in Figure 10.

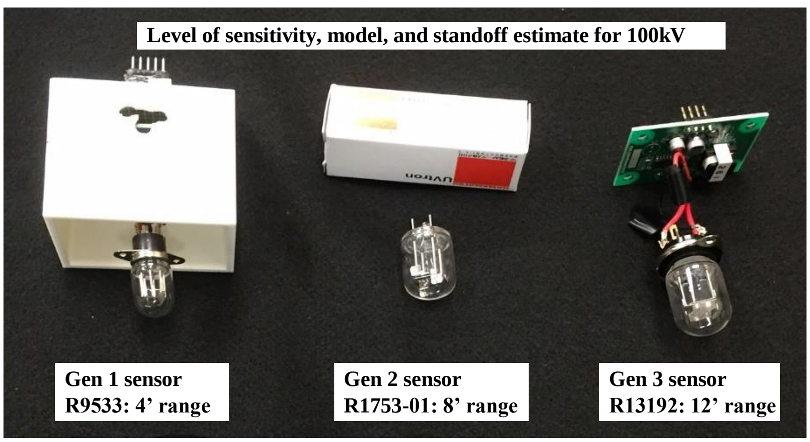


**Figure 9. Left: The Hamamatsu line of compact UV sensors from the first generation, which can sense a 100kV corona at four feet of standoff, to the third generation (R13192), which can sense a 100 kV corona at a distance of approximately twelve feet.**

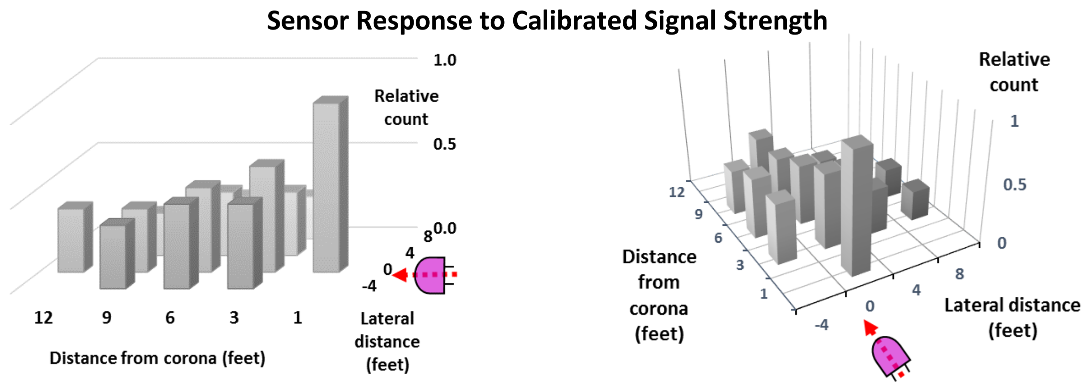


**Figure 10. Sensitivity profile of the R13192 photoelectric UV sensor, with the corona generator set to approximate a 100 kV corona. At left is a top oblique view of the profile, and at right is a moderately elevated side view. The sensor location is indicated by the arrow and bulb icon.**

## B. Airborne Standoff Distance and Corona Generator Settings

For brevity, we use sGPS to indicate single-ended GPS, and dGPS to indicate differential GPS [12] in this report.

To achieve adequate sensing, a UAV equipped with a third generation photoelectric UV sensor must carry it to a distance of 12 feet or less from the source of 100 kV corona emission. This can be achieved safely for manual flight (i.e., using the joysticks on an RC transmitter) if the pilot continuously controls the standoff distance. For autonomous flights, GPS or other geolocation methods are needed to enforce standoff.

Twelve feet is only slightly greater than the accuracy of standard, consumer-grade sGPS. GPS accuracy is a statistical quantity, meaningful only for a percentage of measurements. Using 95% as the statistical allowance, sGPS accuracy is about six feet in latitude and longitude and approximately 2 times poorer in altitude accuracy [13]. UAV autopilots commonly use a barometer for altitude correction of sGPS. Figure 11 illustrates this challenge: inexpensive sGPS introduces an envelope of positional uncertainty around the UAV that is a large fraction of the corridor volume needed for accurate measurement.

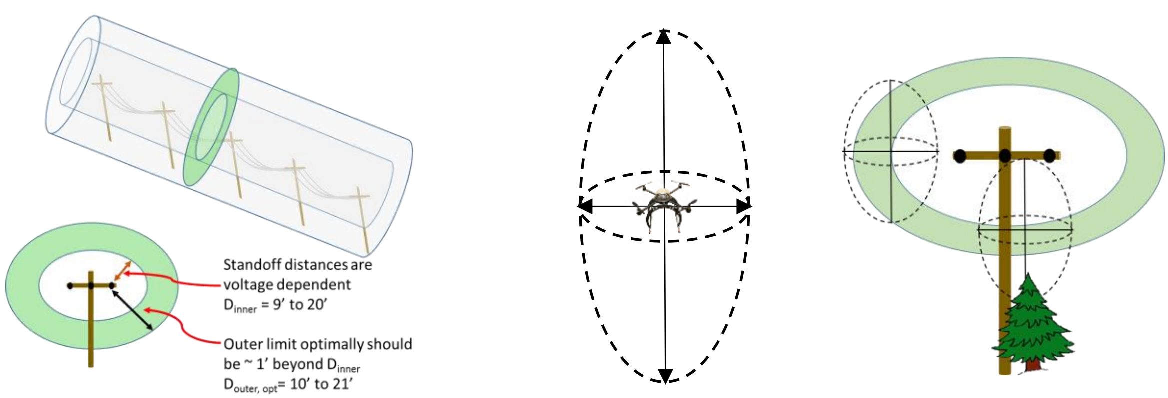


**Figure 11. Flight volume (left), positional uncertainty (middle), and sensing pose (right). With single-ended GPS, the positional uncertainty is a large fraction of the desired standoff distance.**

An increase in accuracy is possible with differential GPS (dGPS), in which two single-ended receivers, one on the UAV and another on the ground station, compute a relative location. When operating with full fidelity, dGPS has a positional uncertainty on the order of centimeters. We pursued this technology throughout 2016. Our research confirmed that dGPS can, in the best case, deliver this accuracy, but that this ideal level of fidelity was intermittent.

For example, when not attached to a UAV, full accuracy was possible, but when mounted on the aircraft it was rare. In fact, the autopilot that we used (Pixhawk controller [14], running Arducopter 3.3) will not allow arming and takeoff of a UAV if dGPS accuracy is poor, and we could never achieve the required accuracy for arming and takeoff with dGPS guidance.

Over the course of the year, two other NASA research groups attempted to adopt low-cost dGPS technology with varied success. Significantly, if arming and takeoff were successful and dGPS "lost lock" (i.e., failed to meet a threshold level of accuracy) during the flight, the autopilot would shift to an onboard backup single-ended sGPS. When this shift occurred, the spatial control envelope of the UAV would expand from centimeters to meters, and the aircraft would jump into a new position estimated from the (low accuracy) single-ended sGPS. This jump, while not catastrophic a) is jarring and can lead to pilot overreaction, and b) almost always resulted in a mission abort due to autopilot safety protocols. At present, the level of confidence in dGPS units small enough to fly on a UAV is very low. To obtain NASA flight safety permissions for the Chester flights, we had to remove differential GPS from the research program, because of concerns about abrupt position changes during the UAV flight.

To compensate for sGPS inaccuracy, standoff distance for autonomous flights was set to 20 feet (though a standoff distance of 12 feet was used for manual flights; Figure 12). At a twenty foot standoff distance, even a shift of six feet (from the center to the outer limit of the positional accuracy envelope) would not result in a collision of the UAV into the inspected structure. The corona generator output had to be increased above the 100 kV calibration output level to be detectable at a 20 foot distance. Until the method described in this report is verified on actual corona faults, we cannot state with certainty that the technologies tested in this study will produce diagnostic results. We can claim that the method has practicality and relevance, but not adequacy, until it is tested successfully on a calibrated UV source or an actual fault. Improved positional accuracy is critical to proving adequacy.

Using only sGPS positional accuracy as a guide, we can conclude (right image of Figure 14) that flying beneath power lines is not safe, and that flying to the side (as done in this study) is safe but not adequate. Flying over lines using sGPS for navigation is safe, but adequacy is even more problematic because sGPS vertical positional uncertainty is 2X greater than sGPS horizontal positional uncertainty. If the vertical positional uncertainty can be reduced, then flying over lines or above and to the side of them is possible (Figure 13). We did not thoroughly quantify the accuracy of the autopilot's fusion of sGPS and barometer, but the results from flights S2_3, S2_4, and S2_5 indicate that the required vertical accuracy is available in some circumstances.

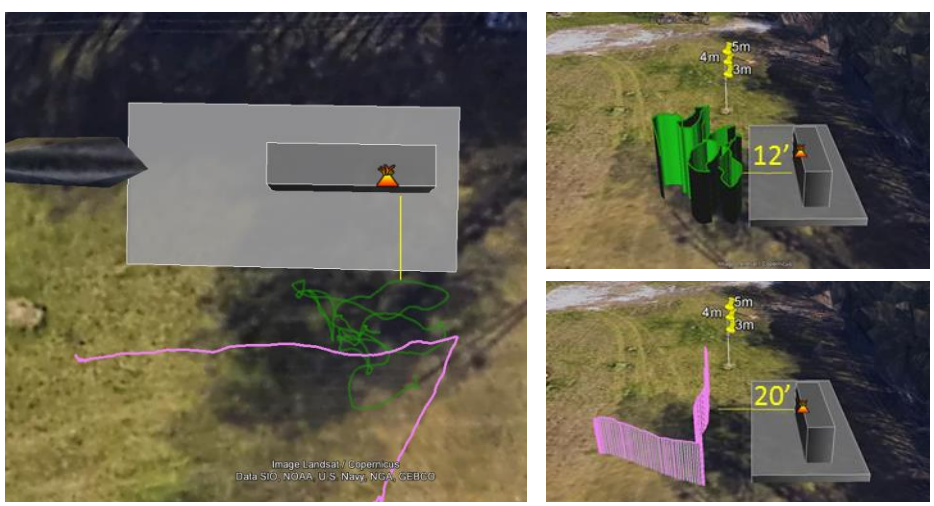


**Figure 12. Distance from corona source in manual and autonomous flights. Top and side views for flights S1_1 (green) and S1_3 (pink) are shown. Due to GPS uncertainty, while manual flights approached the 12 foot calibration distance, autonomous flights approached no closer than 20 feet (horizontal yellow line). To compensate, the corona generator output was increased above calibration levels. The substation structure and its concrete pad are rendered manually and the corona generator location is indicated by an orange icon. *©Map data: Google, DigitalGlobe & NASA***

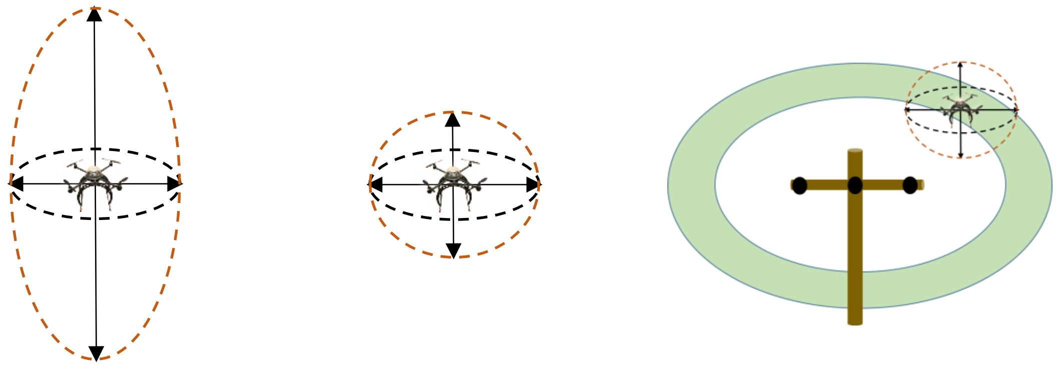

**Figure 14. Reducing vertical position uncertainty. Left: sGPS uncertainty. Middle: Barometric or laser altimeter correction of vertical position estimate, fused with sGPS horizontal position estimate. Right: An example safe position that results from improved vertical accuracy.**

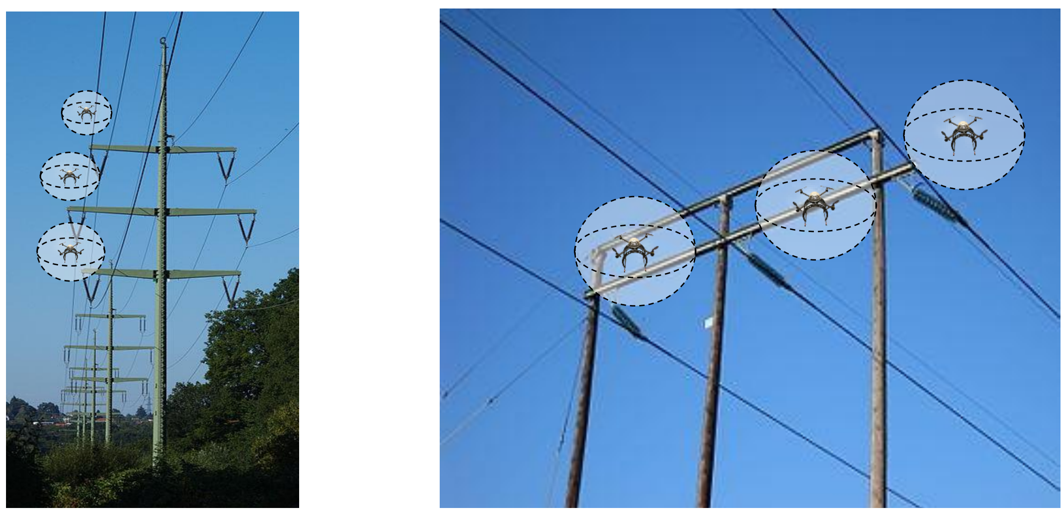

**Figure 13. Examples of inspection positions that take advantage of reduced vertical uncertainty**

### C. Advancements for repeated autonomous flights

Multiple technology developments are required to advance from manual flights to the repeatable autonomous needed to realize a self-diagnosing grid. In this section, we discuss the outlook for two of them: UAV location determination and compact fault sensing.

*1. Improving positional accuracy*

One technology gap that prevents autonomous UAV inspection flights is positional accuracy. Neither sGPS nor current low-cost dGPS can close the gap, in our experience. As discussed above, single-ended GPS is not accurate enough to approach a 100 kV corona close enough to measure its UV emission with current compact sensors. While the two low-cost differential GPS systems that we tested are small enough to fly on an under-55-lb UAV, they fail intermittently, which can result in abrupt position changes during flight.

Some possible strategies to advance autonomous measurement adequacy given the shortcomings of GPS are:

a. Use autonomous flight segments whenever possible to safely approach the transmission structure, supplemented with manual flights as needed
b. Equip the UAV with reliable (presumably high-cost) differential GPS, or develop diagnostics that alert the pilot if high-accuracy flight is not available
c. Develop alternative positioning technology such as lidar, sonar, radar or stereo vision

<u>Autonomous vs. manual flights and safe separation</u>

In manual flights, standoff distances adequate for UV sensing is attainable if a pilot has a good view of the UAV standoff from the inspection structure. In all flights described in this report, the pilot position was chosen to ensure a good view. We designed autonomous flight paths (i.e., waypoints) sufficient for successful inspection without manual pilot intervention. Due to the horizontal positional uncertainty of single-ended GPS, we were forced to adopt a conservative and inadequate horizontal standoff distance for autonomous flights (Figure 12).

Flights above (rather than to the side of) inspection structures can take advantage of the smaller vertical uncertainty afforded by non-GPS altimetry (Figure 15). The placement of static wires, which are sometimes poorly resolved in lidar imagery, is an important constraint to consider in developing this approach.

<u>Invest in more accurate GPS or diagnostics</u>

We tested two hobby-grade differential GPS systems that cost $1000 or less, and avoided more mature systems that cost $5000 or more, since those systems cost more than the UAV itself. High-grade differential GPS packages may offer greater stability and uptime than the two packages we tested.

In the future, low-cost, compact systems can in principle be supplemented with diagnostics that indicate whether precision flight is possible from minute to minute. We find signals that may serve as such a diagnostic in the raw output of the dGPS systems that we tested, but they are not currently available to the pilot.

<u>Develop alternative positioning technology</u>

Other sources of position determination may close the gap that currently hinders autonomous UAV inspection flights. Compact sonar detectors are available with specifications that claim accurate distance measurement up to about 20 feet. Lidar has a far greater inherent range, but compact units with suitable size, power, and spatial resolution are not assured. In general, there is a tradeoff: a lidar system has a) small size and power consumption, or b) high spatial resolution, but not both. Radar, similarly, is inherently capable, but so far no compact units are in widespread use. The hardware required for visual ranging using stereo camera streams or a time sequence of images (phodar) is quite compact, but the real-time computation needed to make it useful requires processing power that is only now becoming available in a form that is compact enough to install on a small UAV. Techniques that fuse multiple sensors (see for example [15][16]) are developing rapidly.

*2. Increasing detector sensitivity*

There are two methods to enhance the sensor range. First, optical focusing with a UV-transparent lens approximately doubles the detection distance [17][18]. However, quartz lenses are heavy and cost much more than the sensor, and the field of view for practical lenses is limited to about 10 degrees. Second, optical focusing with a UV-reflective mirror can increase the detection distance by a factor dependent on the mirror radius and curvature [19][20]. As with lens augmentation, mirror augmentation increases sensitivity but decreases the field of view. The design of a UV reflective mirror for UAV-based corona detection should maximize field of view within practical limits of weight, cost, and aerodynamic drag.

## V. Conclusion

In this report, we documented test and measurement flights of a UAV, equipped with a low-cost UV sensor, at two de-energized high-voltage structures. In the measurement flights, the sensor signal was verified with a ground-based commercial corona camera, and the UAV position was monitored on a local ground station laptop. Simultaneously, the laptop transmitted the UAV position to a remote NASA UTM server that tracked it in the US air space.

Navigation and sensing technology gaps were identified and future improvements to mitigate them were recommended. One technology gap that prevents precision autonomous UAV inspection flights is positional accuracy. Neither single-ended GPS nor current low-cost differential GPS can close this gap. The two low-cost differential GPS systems tested are small enough to fly on an under-55-lb UAV, but fail intermittently; this can result in abrupt position changes during the flight. Improvements in UAV position determination technology are needed for general application of this method.

Increasing the range of onboard UV sensors would lessen the need for precision position determination. If the standoff distance can be doubled from 12 feet to 24 feet with compact optics, then sGPS would be sufficiently accurate. With a sensitivity improvement high enough to allow a safe standoff distance using affordable positioning technology, a fleet of UAVs equipped with compact UV sensors could serve as an autonomous detection capability that enables a self-diagnosing power grid.

## VI. Acknowledgments

We are grateful to the following NASA Langley colleagues for early discussions about the various facets of this mission: Tom Vranas (UAV selection and testing), Scott Dorsey (ultraviolet sensing), Taumi Daniels (corona physics), Kelly Hayhurst and Jill Brown (mission and regulatory framework), and Evan Dill and Robert McSwain (differential GPS). This work could not have been accomplished without the close partnership with and generous assistance from

Steve Eisenrauch, Amanda Palmore and their colleagues of Dominion Virginia Power. Fabio Bologna and Andrew Philips of the Electric Power Research Institute, Charlotte, NC, supplied a 100 kV calibration corona and associated imagery, and invaluable advice. James Hubbard of the National Institute of Aerospace and the University of Maryland provided advice about the mission. This work was performed with support from the NASA Safe Autonomous Systems Operations program, under the direction of Sharon Graves.

## VII. References

[1] Blanks, Mark. "UAS Applications." *Introduction to Unmanned Aircraft Systems*, 2nd ed., CRC Press, Boca Raton, 2016, Ch. 2, 19.
[2] Knight, R. "The Power of UAS." *Inside Unmanned Systems*. January-February 2017, p. 31
[3] Ito, R. "Unmanned Aircraft Systems Pass Field Tests with Flying Colors." *Epri Journal*, November-December 2017, p. 16.
[4] Wolf, Gene. "The Drone Advantage." *Transmission and Distribution World*. Vol. 68 No. 4, April 2016, p. 106
[5] Matikainen, L., Lehtomäki, M., Ahokas, E., Hyyppä, J., Karjalainen, M., Jaakkola, A., Kukko, A. and Heinonen, T., "Remote sensing methods for power line corridor surveys." *ISPRS Journal of Photogrammetry and Remote Sensing*, Vol. 119, 2016, pp. 10-31.
[6] Menendez, O.A., Perez, M., and Cheein, F.A.A., "Vision based inspection of transmission lines using unmanned aerial vehicles." *2016 IEEE International Conference on Multisensor Fusion and Integration for Intelligent Systems (MFI)*, Baden-Baden, 2016, pp. 412-417.
[7] Schubert, M., and Moore, A.J., "Morphological processing of ultraviolet emissions of electrical corona discharge for analysis and diagnostic use." *Applied Optics* Vol. 55, No. 7, 2016, pp. 1571-1572.
[8] Warashina, H. "Ultraviolet detector", US Patent 5959301 A, Sep 28, 1999.
[9] Moore, A.J., Schubert, M. and Rymer, N., "Autonomous Inspection of Electrical Transmission Structures with Airborne UV Sensors-NASA Report on Dominion Virginia Power Flights of November 2016." NASA Technical Memo 2017-219611 (2017).
[10] Prevot, T., Rios, J., Kopardekar, P., Robinson III, J. E., Johnson, M., and Jung, J., "UAS traffic management (UTM) concept of operations to safely enable low altitude flight operations." *16th AIAA Aviation Technology, Integration, and Operations Conference*, Washington, D.C., 2016. p. 3292
[11] Hamamatsu Flame Sensor UV TRON, Hamamatsu Photonics K.K., Electron Tube Center, Shimokanzo, Toyooka-village, Iwata-gun, Shizuoka-ken, 438-0193, Japan
[12] Parkinson, Bradford W., and Per K. Enge. "Differential GPS." *Global Positioning System: Theory and applications 2* (1996): 3-50.
[13] Civil Report Card On GPS Performance Nov 2016. (2016, December). Retrieved March 15, 2017, from http://www.nstb.tc.faa.gov/reports/ReportCards/2016 11.pdf
[14] Meier, Lorenz, Dominik Honegger, and Marc Pollefeys. "PX4: A node-based multithreaded open source robotics framework for deeply embedded platforms." *2015 IEEE International Conference on Robotics and Automation (ICRA)*, Seattle, WA, 2015, pp. 6235-6240.
[15] Zhang, J, and Singh, S., "Enabling Aggressive Motion Estimation at Low-drift and Accurate Mapping in Real-time*." IEEE Intl. Conf. on Robotics and Automation (ICRA)*. Singapore, May 2017, pp. 5051-5058.
[16] Dill, E., and Uijt de Haag, M., "Integration of 3D and 2D imaging data for assured navigation in unknown environments." *IEEE/ION Position, Location and Navigation Symposium*, Indian Wells, CA, USA, 2010, pp. 285-294.
[17] Kim, Y. S., and Shong, K. M., "The Characteristics of UV Strength According to Corona Discharge From Polymer Insulators Using a UV Sensor and Optic Lens," in *IEEE Transactions on Power Delivery*, vol. 26, no. 3, July 2011, pp. 1579-1584.
[18] Kim, Y. S., and Shong, K. M., "Measurement of corona discharge on polymer insulator through the UV rays sensor including optical lens," *2010 10th IEEE International Conference on Solid Dielectrics*, Potsdam, 2010, pp. 1-4.
[19] Engelhaupt, D. E., Reardon, P. J., Blackwell, L., Warden, L., & Ramsey, B. D. "Autonomous long-range open area fire detection and reporting." *Defense and Security*. International Society for Optics and Photonics, 2005, pp. 164-175.
[20] Engelhaupt, D.E., "Optical flame detection system and method." U.S. Patent No. 7,541,938. 2 Jun. 2009.